

Article

Grain Refinement and Improved Mechanical Properties of EUROFER97 by Thermo-Mechanical Treatments

Giulia Stornelli ^{1,*} , Andrea Di Schino ² , Silvia Mancini ³, Roberto Montanari ¹ , Claudio Testani ⁴ 
and Alessandra Varone ¹

¹ Dipartimento di Ingegneria Industriale, Università di Roma "Tor Vergata", 00133 Rome, Italy; roberto.montanari@uniroma2.it (R.M.); alessandra.varone@uniroma2.it (A.V.)

² Dipartimento di Ingegneria, Università di Perugia, Via G. Duranti 93, 06125 Perugia, Italy; andrea.dischino@unipg.it

³ RINA Consulting Centro Sviluppo Materiali, Via di Castel Romano 100, 00128 Rome, Italy; silvia.mancini@studenti.unipg.it

⁴ CALEF-ENEA CR-Casaccia, Via Anguillarese 301, S. Maria di Galeria, 00123 Rome, Italy; claudio.testani@consorziocalef.it

* Correspondence: giulia.stornelli@students.uniroma2.eu

Abstract: EUROFER97 steel plates for nuclear fusion applications are usually manufactured by hot rolling and subsequent heat treatments: (1) austenitization at 980 °C for 30 min, (2) rapid cooling and (3) tempering at 760 °C for 90 min. An extended experimental campaign was carried out with the scope of improving the strength of the steel without a loss of ductility. Forty groups of samples were prepared by combining cold rolling with five cold reduction ratios (20, 40, 50, 60 and 80%) and heat treatments at eight different temperatures in the range 400–750 °C (steps of 50 °C). This work reports preliminary results regarding the microstructure and mechanical properties of all the cold-rolled samples and the effects of heat treatments on the samples deformed with the greater CR ratio (80%). The strength of deformed samples decreased as heat treatment temperature increased and the change was more pronounced in the samples cold-rolled with greater CR ratios. After heat treatments at temperature up to 600 °C yield stress (YS) and ultimate tensile strength (UTS) of samples deformed with CR ratio of 80% were significantly larger than those of standard EUROFER97 but ductility was lower. On the contrary, the treatment at 650 °C produced a fully recrystallized structure with sub-micrometric grains which guarantees higher strength and comparable ductility. The work demonstrated that EUROFER97 steel can be strengthened without compromising its ductility; the most effective process parameters will be identified by completing the analyses on all the prepared samples.

Keywords: EUROFER97; RAFM steels; thermo-mechanical treatments; microstructure; dislocation density; recrystallization



Citation: Stornelli, G.; Di Schino, A.; Mancini, S.; Montanari, R.; Testani, C.; Varone, A. Grain Refinement and Improved Mechanical Properties of EUROFER97 by Thermo-Mechanical Treatments. *Appl. Sci.* **2021**, *11*, 10598. <https://doi.org/10.3390/app112210598>

Academic Editor: Emmanuele Peluso

Received: 15 October 2021

Accepted: 9 November 2021

Published: 11 November 2021

Publisher's Note: MDPI stays neutral with regard to jurisdictional claims in published maps and institutional affiliations.



Copyright: © 2021 by the authors. Licensee MDPI, Basel, Switzerland. This article is an open access article distributed under the terms and conditions of the Creative Commons Attribution (CC BY) license (<https://creativecommons.org/licenses/by/4.0/>).

1. Introduction

Reduced activation ferritic-martensitic (RAFM) steels, a variant of conventional ferritic-martensitic steels, were developed to be used as structural materials in future nuclear fusion reactors and nuclear fission reactors of generation IV [1,2].

Compared to austenitic stainless steels, RAFM steels are preferred in high radiation density applications, due to their high thermal conductivity, relatively low thermal expansion and greater resistance to radiation damage [3–5].

One of the main requirements for the construction of nuclear fusion reactors is to ensure easy storage of radioactive waste after the decommissioning of the nuclear plant [6]. In this regard, the key feature of RAFM steels is that some chemical elements, typically present in the commercial Cr-Mo ferritic-martensitic steels [7–9], have been replaced with metallurgically equivalent elements, characterized by short radioactive decay times [10,11].

In particular, Mo was replaced with W and Nb with Ta and V. Likewise, the concentration of Ni, Cu, Al, Co and other impurity elements, with high long-term radioactivity, was kept as low as possible [12–14].

EUROFER97 steel is the reference RAFM steel in Europe for test blanket modules (TBMs) in the ITER reactor [14–16], as well as a possible candidate material for the first wall in the DEMO reactor and other highly stressed sections as a blanket, vessel and divertor [17–20]. It is produced through a hot-rolling process followed by three heat treatment steps [21]: (1) austenitization at 980 °C for 30 min, (2) rapid cooling in air and (3) tempering at 760 °C for 90 min; henceforth, this treatment condition will be referred to as “standard” in comparison to the variants tested during the present activity.

EUROFER97 exhibits good weldability and the original microstructural and mechanical characteristics in molten and heat affected zones can be in large part recovered after suitable post-welding heat treatments [22].

Under irradiation EUROFER97 steel has good mechanical performances in the temperature range between 350 °C and 550 °C [23–25] and several studies have been performed aimed to extend the operating temperature range. A possible solution to raise the maximum operating temperature, above 550 °C, is a variant of EUROFER97 steel reinforced by dispersion of oxide (ODS) [26]. EUROFER97-ODS is produced by mechanical alloying of yttrium oxide powders (Y_2O_3 at 0.3 wt.%) [27,28]. The presence of nano-oxide, finely dispersed in the microstructure, inhibits grain boundary sliding and tends to retard grain growth at high temperature. In this way, the improved thermal stability leads the operating temperature to increase up to about 600–650 °C [29–33]. Moreover, the dispersion of oxide nanoparticles strengthens the steel [34] and reduces the irradiation swelling because it acts as a trap for the defects induced by neutron radiation.

The lower temperature limit at 350 °C is mainly connected to a loss of ductility due to the increase in hardness, induced by defects produced by the neutron irradiation [7] and clustering of Cr atoms [35–37]. In general, grain refinement at low temperature increases material strength, but the ductility is decreased as a result of increased dislocation density [38]. At high temperature, grain refinement leads to increased strength without losing ductility [39].

The scope of this work was to develop a thermo-mechanical treatment that improves the mechanical performances of EUROFER97 without reducing its the ductility, through the refinement of microstructure [40–42]. Moreover, a finer microstructure has other advantages in nuclear applications [41] because grain boundaries act as sinks for the Frenkel pairs produced by irradiation and traps for He and H atoms [43,44]. Therefore, a process that leads to grains of lower size would also promote better irradiation strength and reduced He/H susceptibility.

The microstructural evolution of ferritic steels under different thermo-mechanical treatments has been discussed in [45,46]. In the literature, many studies have investigated the effect of different thermo-mechanical treatments (TMTs) on the irradiation resistance of EUROFER97 steel and, various strategies have been adopted to refine the microstructure (e.g., [47–50]). Karthikeyan et al. [51] and Pilloni et al. [52] showed that a double austenitization treatment refines the prior austenitic grain (PAG) and increases toughness.

On these grounds we carried out an extended experimental campaign, aiming to improve the strength of the steel through microstructure refining without introducing detrimental effects on its ductility [53]. Therefore, 40 groups of samples were prepared by combining five cold-rolling reduction (CR) ratios (20, 40, 50, 60 and 80%) and eight heat treatments at temperatures from 400 °C to 750 °C (steps of 50 °C). This work reports preliminary results regarding the microstructure and mechanical properties of all the cold-rolled samples and the effects of heat treatments only on the samples deformed with CR ratio of 80%. The results are discussed in comparison to the properties and characteristics of the steel prepared through the standard process.

2. Materials and Methods

The nominal chemical composition of EUROFER97 steel is reported in Table 1 [1].

Table 1. Nominal chemical composition of EUROFER97 steel (wt.%) (Fe to balance) [1].

Cr	C	Mn	V	W	Ta	Ti	N
8.93	0.12	0.47	0.2	1.07	0.14	0.009	0.018
P	S	B	Si	Nb	Mo	Ni	Cu
<0.005	0.004	<0.001	0.006	0.002	0.0015	0.002	0.003

A plate of EUROFER97 steel prepared according to the standard treatment was cut in five parts and each part was cold rolled with a different cold reduction (CR) ratio: 20, 40, 50, 60 and 80%. From each cold rolled sheet specimen was machined and then annealed at eight different temperatures from 400 °C to 750 °C (steps of 50 °C), for 1 h in an argon atmosphere. The heat treatment temperatures were chosen to operate in the ferritic field [41]. By combining cold rolling ratio and treatment temperature, 40 different sets of specimens were prepared.

The microstructure of EUROFER97 samples was examined by high-resolution electron scanning microscopy (FE-SEM- Zeiss, Gemini Supra 25, Jena, Germany), light microscopy (LM- Union Optical Co., Ltd., Tokyo, Japan) and X-ray diffraction (XRD- PW 1729, Philips, Eindhoven, The Netherlands). SEM and LM observations were carried out after mechanical polishing of the sample surface and etching by means of Vilella reagent.

XRD patterns were collected in the 2θ angular range 15–60° by using the Mo-K α radiation ($\lambda = 0.070926$ nm) with 2θ steps of 0.05° and counting time in steps of 2 s. From the relative intensities of the peaks in each pattern the crystalline texture was evaluated. The dislocation density ρ was determined from precision peak profiles recorded with 2θ steps of 0.005° and counting time in steps of 4 s. After background subtraction the peak profiles were fitted by Lorentzian curves to eliminate the K α 2 component, then the full width at half maximum (FWHM) was corrected from the instrumental broadening to get the total broadening (β_T) that is the sum of two contributions due to the size (D) of coherently diffracting domains (β_D) and the micro-strains (β_ϵ) induced by dislocations:

$$\beta_T = \beta_D + \beta_\epsilon = \frac{0.89\lambda}{D \cos \theta} + 2\epsilon \tan \theta \quad (1)$$

where θ is the Bragg's angle of the XRD peak. To determine the two contributions, β_D and β_ϵ , the Cauchy procedure was used by plotting $\beta_T \cos \theta / \lambda$ vs. $\sin \theta / \lambda$.

The dislocation density ρ was then calculated through the Williamson–Smallman relationship [54]:

$$\rho = \frac{\Xi \epsilon^2}{F b^2} \quad (2)$$

where $\Xi = 16.1$ a constant, $F \approx 1$ a factor depending on the interaction of dislocations and $b = 0.248$ nm the modulus of Burgers vector.

The mechanical properties were investigated through Vickers hardness and FIMEC (Flat-top cylinder Indenter for Mechanical Characterization) tests. FIMEC is an instrumented indentation test employing a cylindrical punch and its typical characteristics have been described in detail in many papers (e.g., see [19,55,56]). In the present study FIMEC was used to measure the yield stress YS and the reported data are the mean values of three tests.

Vickers hardness tests were made by means of a HV50 (Remet, Bologna, Italy) instrument by using a load of 5 kg. Three hardness tests were made on each sample in the central zone of the longitudinal cross-section.

Based on the hardness results, tensile tests were performed on EUROFER97 steel deformed with CR of 80% after heat treatments at 400 °C, 500 °C, 600 °C and 650 °C. Flat probes were machined along the transverse direction and tensile tests were carried out according to ASTM E8 standard using a servo-mechanical MD 100 tensile machine (MAYES, China). A drawing of a probe used in tensile tests is shown in Figure 1. For each material, three tests were carried out and the curves showed a high reproducibility.

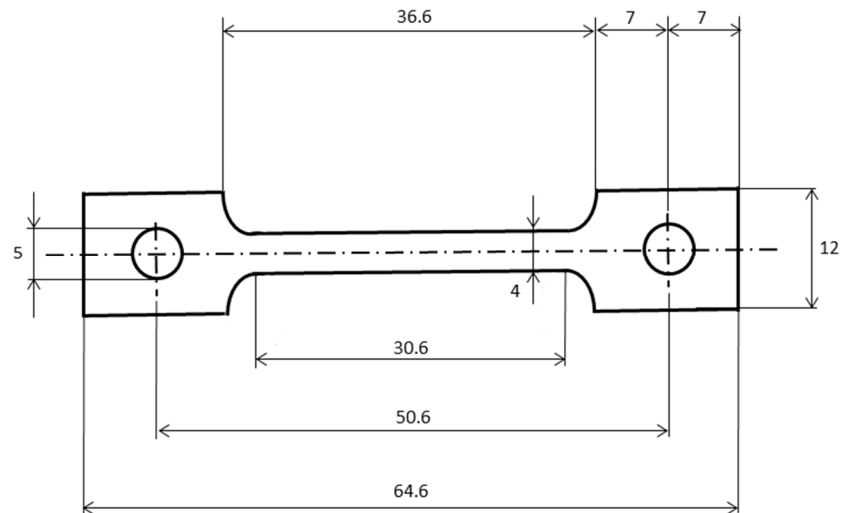


Figure 1. Schematic drawing of a typical probe used in tensile tests (dimensions are expressed in millimeters).

3. Results and Discussion

3.1. Work-Hardening Behavior of EUROFER97 Steel

The effect of cold rolling on the EUROFER97 microstructure is shown in the SEM images of Figure 2. Figure 2a shows the microstructure of EUROFER97 steel after the standard treatment consisting of tempered martensite with carbides decorating the prior austenitic grains (PAGs) and former lath packet boundaries. A detailed analysis of carbide types, chemical composition, morphology and spatial distribution confirmed results already reported in the literature (e.g., [57,58]). Coarse $M_{23}C_6$ ($M = Cr, W$) carbides decorate the PAG and the boundaries of martensite lath packets while the MX ($M = Ta, V$) carbo-nitrides are finely dispersed inside the lath structure. The micrographs in Figure 2b–f display the microstructures after cold rolling with increasing CR ratio. As expected, the original grains tend to progressively become flat and elongated along the rolling direction and this characteristic becomes more evident with larger CR ratios. As indicated by red arrows in (b), inside some original grains, a population of new grains with size below $\sim 1 \mu m$ forms. For the highest degree of deformation (CR ratio of 80%) the elongated grains were fragmented into new equiaxed grains with mean size of ~ 400 nm.

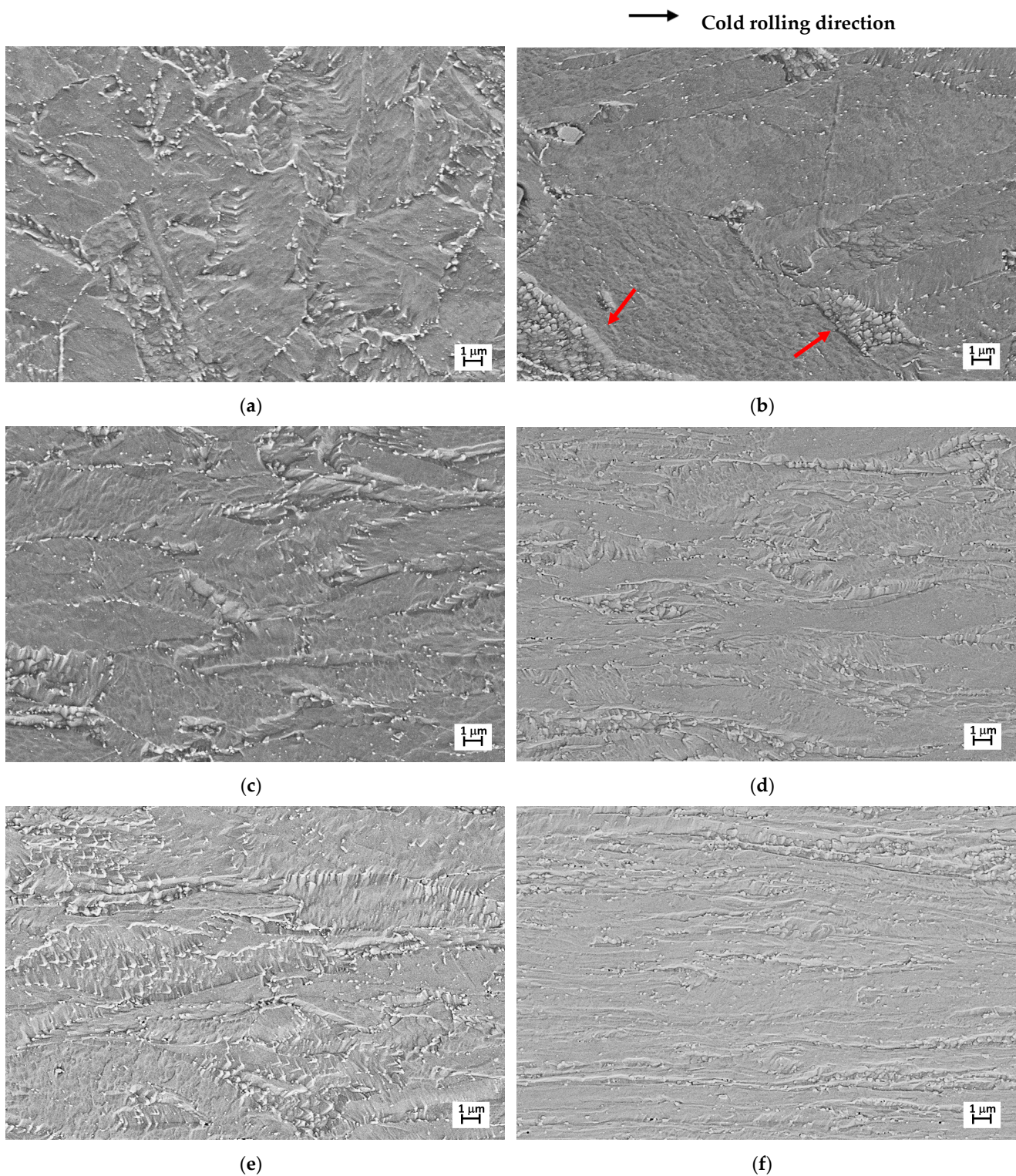


Figure 2. EUROFER97 steel. SEM micrographs of the material in standard condition (a) and after cold rolling with increasing CR ratio: 20% (b), 40% (c), 50% (d), 60% (e) and 80% (f).

Figure 3 shows the XRD patterns of samples prepared by means of the standard treatment and after cold rolling with increasing CR ratios. In each pattern the relative intensities of peaks (see Table 2) provide information about possible textures, i.e., preferred orientations of the grains. The texture can be evaluated by comparing the relative intensities measured in the experiments with those reported in the JCPDS database-file 6-696 [59]

corresponding to Fe with randomly oriented grains. If the examined material has a texture the intensities diverge from such reference values: the greater the difference, the stronger the texture. The samples prepared by means of the standard treatment exhibit a nearly random texture with the presence of a weak [110] component. Such texture then evolves towards a cubic [100] one with a secondary [211] component observed for the greatest CR ratio (80%).

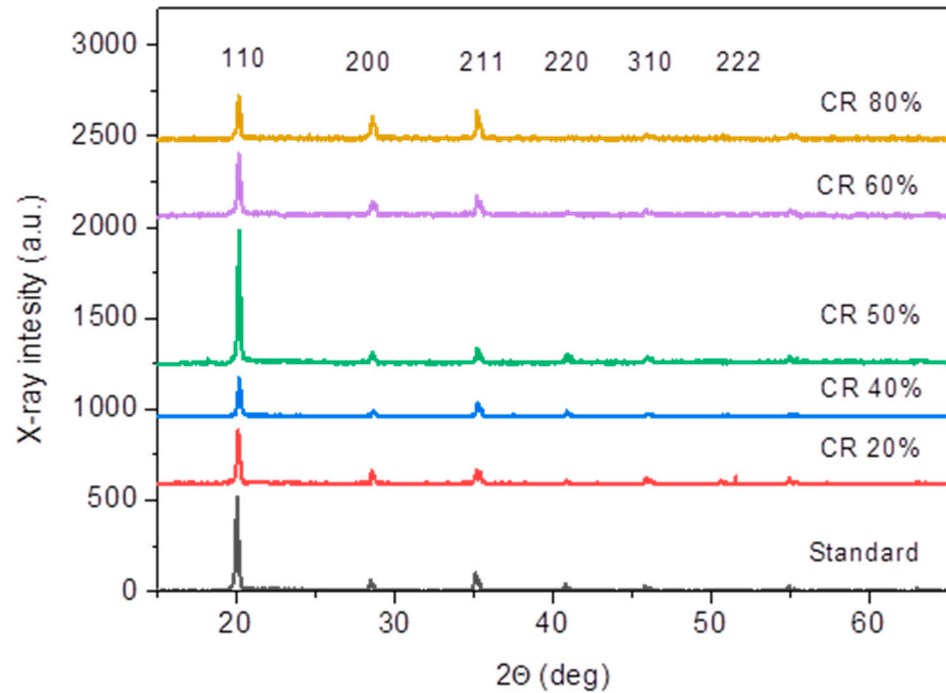


Figure 3. XRD patterns of standard EUROFER97 steel and after cold rolling with increasing CR ratio.

Table 2. Relative intensities of XRD peaks of EUROFER97 steel prepared according to the standard treatment and after cold rolling with increasing CR ratio. The values have been determined from patterns in Figure 3. Data from the file 6-696 of JCPDS database [59] referring to Fe with randomly oriented grains are reported for comparison.

Peaks	110	200	211	220	310	222
JCPDS database-file 6-696	100	20	30	10	12	6
Standard	100	11	20	8	6	-
CR 20%	100	24	27	6	9	5
CR 40%	100	15	38	6	7	4
CR 50%	100	7	12	5	4	-
CR 60%	100	20	30	1	1	1
CR 80%	100	52	63	-	1	1

Another effect of increasing values of CR ratio is the progressive broadening of XRD peak profiles. For example, Figure 4 shows the evolution of the {110} peak; the peak intensities are normalized to make easier the comparison.

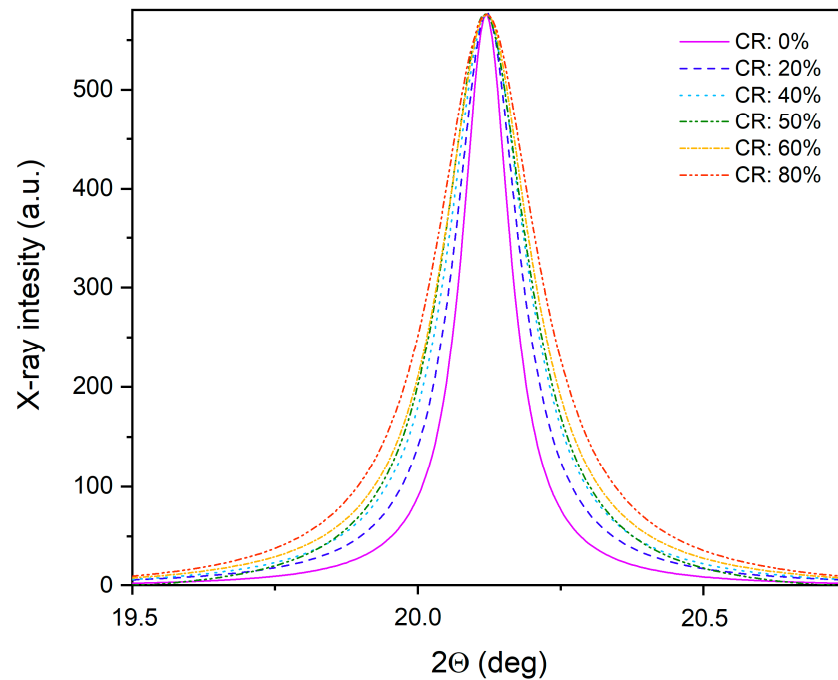


Figure 4. Effect of the cold rolling process on the {100} XRD peak profile of EUROFER97 steel. The broadening of the diffraction peaks is an index of the increase in the dislocation density ρ .

From the analysis of XRD peak profiles the dislocation density were calculated by means of Equation (2) and the results are reported in Figure 5. Some TEM observations have been published in a previous work [20] confirming the XRD data. Dislocation density continuously increases with CR ratio and after 80% deformation it is about two orders of magnitude higher than in the original material. As expected, the ρ increase leads to higher values of hardness and yield strength (Figure 6): the HV_5 and YS values of EUROFER97 steel in the standard condition (CR: 0%) are 200 HV and 470 MPa, respectively, and progressively rise with CR ratio, up to about 300 HV and 690 MPa in the case of 80% cold rolled material.

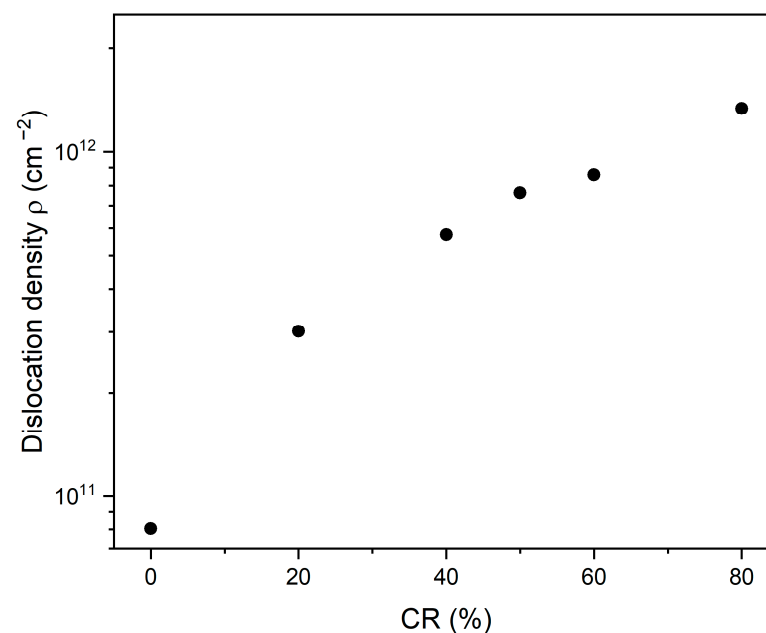


Figure 5. Effect of the CR ratio on the dislocation density ρ .

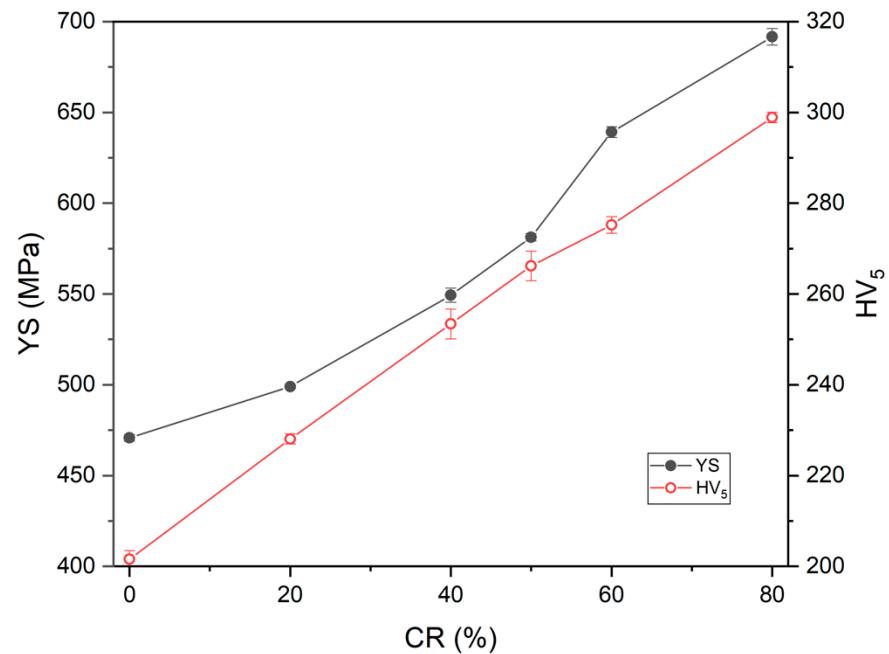


Figure 6. Effect of the CR ratio on hardness HV_5 and yield strength YS measured by means of FIMEC test.

3.2. Recrystallization Behavior of EUROFER97 Steel

Recrystallization takes place in all the heat-treated samples with kinetics depending on treatment temperature and CR ratio. Of course, greater CR ratios promote the start of recrystallization at lower temperatures; however, the samples deformed with CR ratio of 20% recrystallize at the highest temperature examined here (750 °C). This is shown by Figure 7 where a structure of new grains of very small size (~ 300 nm) can be observed.

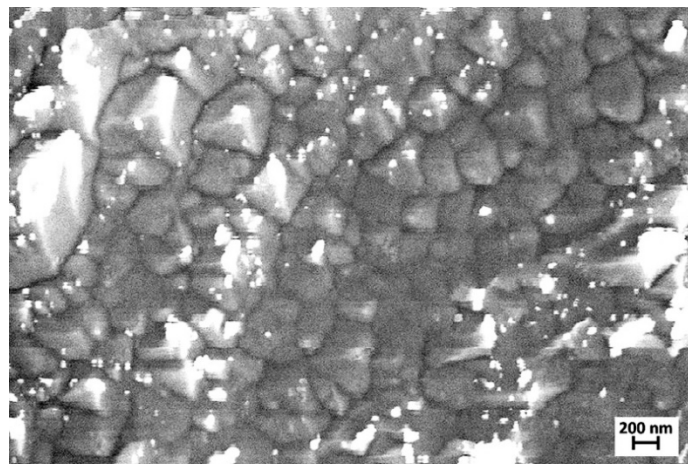


Figure 7. EUROFER97 cold-rolled with a CR ratio of 20% and heat-treated at 750 °C for 1 h.

In this work, attention was focused on the steel cold-rolled with a CR ratio of 80%, and SEM micrographs in Figure 8 illustrate its microstructure evolution following heat treatments at increasing temperature, i.e., 400, 450, 500, 550, 600 and 650 °C. The typical structure with elongated grains originating from cold rolling progressively weakens as treatment temperature increases, and at 650 °C, a population of equiaxed grains of sub-micrometric size can be observed indicating that the primary recrystallization has been completed.

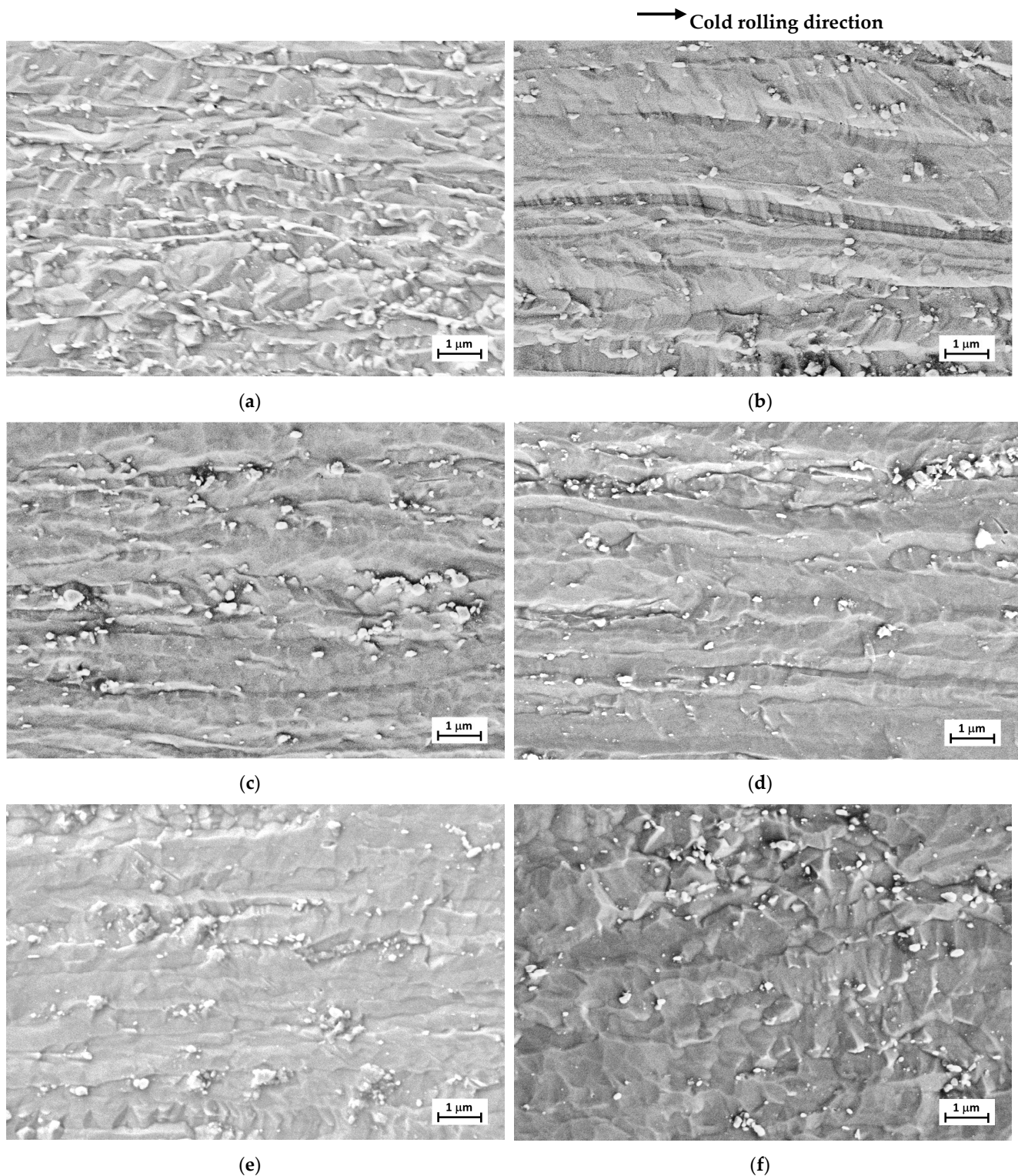


Figure 8. EUROFER97 deformed with a CR ratio of 80% and treated for 1 h at the temperature of: 400 °C (a), 450 °C (b), 500 °C (c), 550 °C (d), 600 °C (e), 650 °C (f).

For higher heat treatments temperatures (700 and 750 °C) some grains undergo an abnormal growth at the expense of neighboring ones (see Figure 9a,b). Some grains, usually aligned along the rolling direction, may reach a size of about 60–70 μm (Figure 9a) while neighboring ones are about 350 nm (Figure 9b). The result is in agreement with those reported by Oliveira et al. [49] who explained the abnormal grain growth as the synergic

effect of high intrinsic grain boundary mobility, size advantage acquired in the early stages of annealing and the presence of local microstructural instabilities such as the dissolution and coarsening of $M_{23}C_6$ carbides.

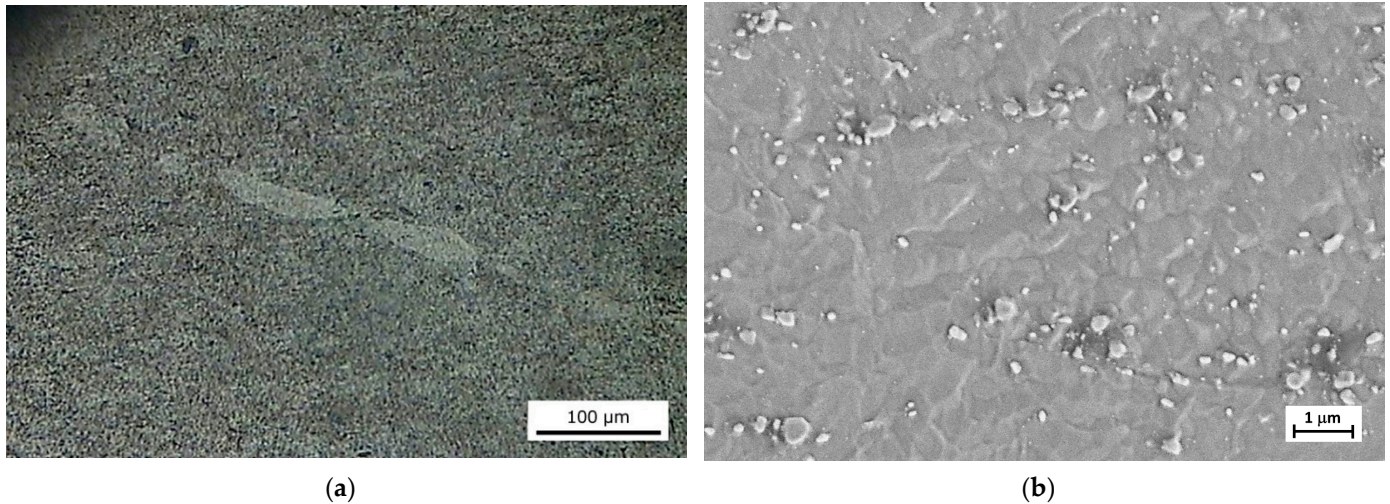


Figure 9. EUROFER97 deformed with a CR ratio of 80% and treated for 1 h at 750 °C. LM micrograph in (a) shows grains of abnormal size which are surrounded by quite smaller grains displayed by the SEM image in (b).

The XRD patterns of EUROFER97 steel cold-rolled with CR ratio of 80% and heat-treated at temperatures in the range from 400 to 750 °C are shown in Figure 10. The relative intensities of XRD peaks determined from the patterns in Figure 10 are reported in Table 3.

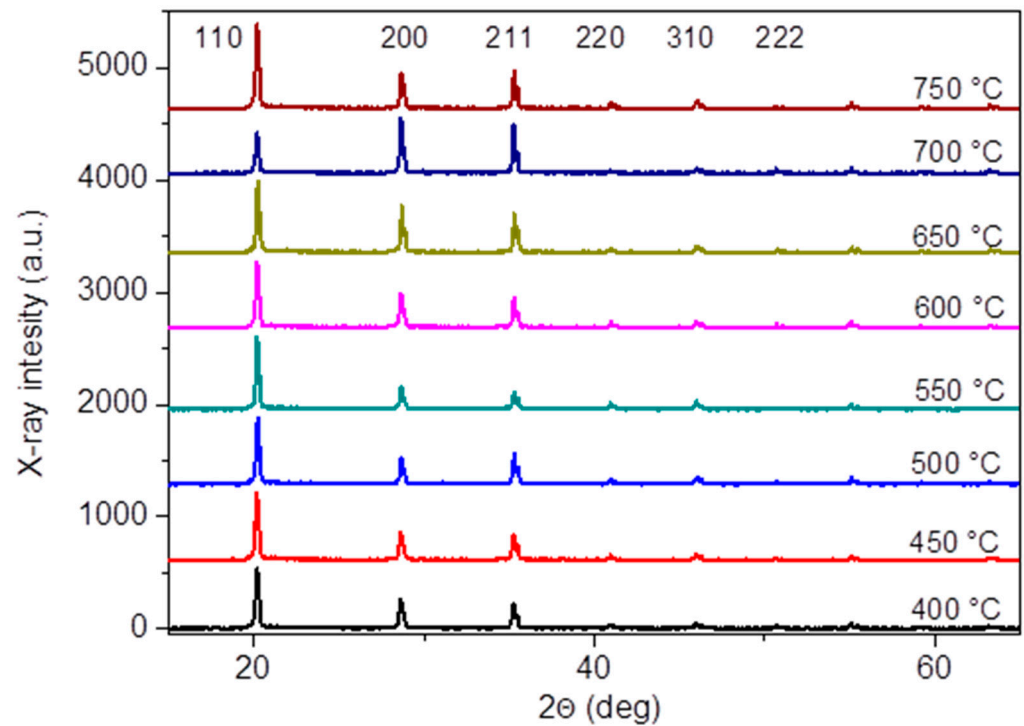


Figure 10. XRD patterns of EUROFER97 steel cold-rolled with CR ratio of 80% and heat-treated at increasing temperatures from 400 to 750 °C with steps of 50 °C.

Table 3. Relative intensities of XRD peaks of EUROFER97 steel cold rolled with CR ratio of 80% and heat-treated for 1 h at the reported temperatures (from 400 to 750 °C in steps of 50 °C). The values have been determined from patterns in Figure 10. Data from the file 6-696 of the JCPDS database [59] referring to Fe with randomly oriented grains and of deformed but not treated steel are reported for comparison.

Peaks	110	200	211	220	310	222
JCPDS database-file 6-696	100	20	30	10	12	6
Standard	100	11	20	8	6	-
CR 80%/not treated	100	52	63	-	1	1
CR 80%/400 °C	100	48	42	8	10	1
CR 80%/450 °C	100	43	38	7	8	1
CR 80%/500 °C	100	41	28	7	8	1
CR 80%/550 °C	100	30	21	6	8	1
CR 80%/600 °C	100	52	45	9	8	3
CR 80%/650 °C	100	66	55	6	9	4
CR 80%/700 °C	73	100	89	6	10	9
CR 80%/750 °C	100	42	44	7	10	4

The samples before heat treatments exhibit a cubic [100] texture with a secondary [211] component which progressively weakens as treatment temperature increases. Such trend observed up to 550 °C indicates that in a first stage of recrystallization the new grains form with the [110] orientation. In a second stage corresponding to the completion of recrystallization the new grains assume the same orientation of old deformed grains thus [100] and [211] texture components are still present.

From the analysis of XRD peak profiles the mean grain size, D , and dislocation density, ρ , have been determined (Figure 11). In the same figure the values of the not-treated steel (N.T.) are displayed for comparison.

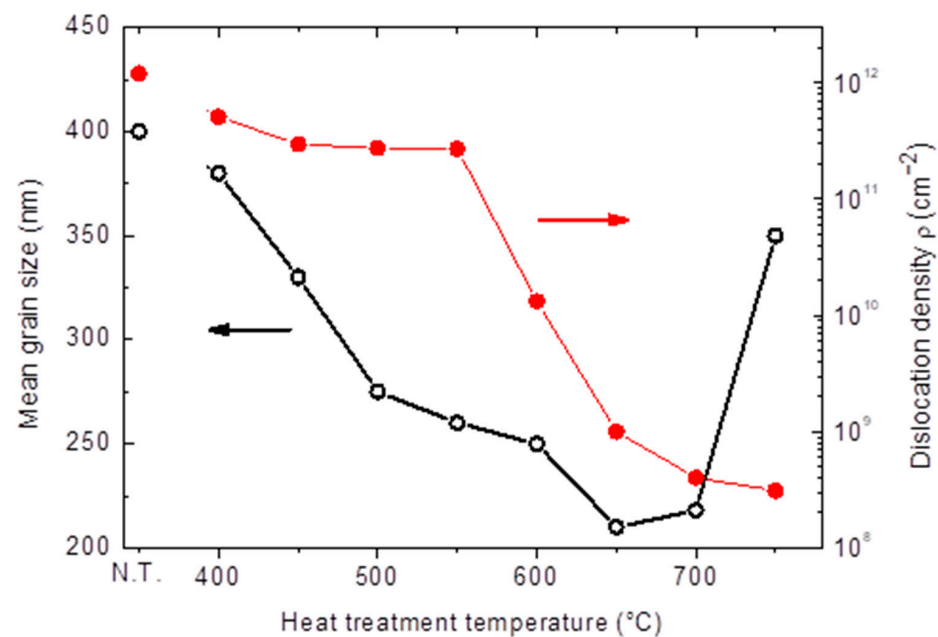


Figure 11. Mean grain size, D , and dislocation density, ρ , determined from the analysis of XRD peak profiles of the steel cold-rolled with a CR ratio of 80% and heat-treated at temperatures in the range 400–750 °C (step 50 °C).

As treatment temperature increases, the dislocation density exhibits a continuously decreasing trend that is the consequence of the formation of new grains free from defects during recrystallization.

The mean grain size has an analogous behavior up to 650 °C because the heavily deformed matrix of the steel has a large number of preferred nucleation sites for new grains. Many nucleation sites and slow growth due to the relatively low temperature produce a population of grains of small size. Above 650 °C grain growth occurs thus an increase in mean grain size can be observed. XRD results are in agreement with SEM observations displayed in Figures 8 and 9.

The effect on hardness of heat treatments for 1 h at eight temperatures on samples submitted to cold rolling with five CR ratios is displayed in Figure 12; the value of standard EUROFER97 is shown for comparison.

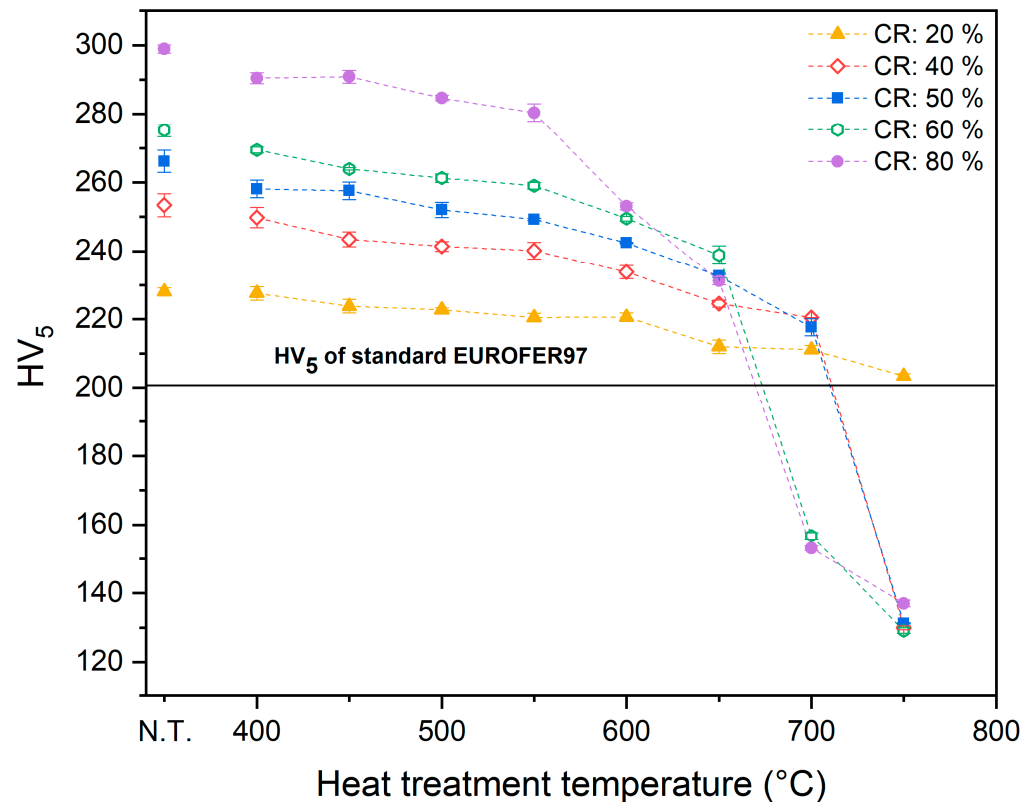


Figure 12. Effect of the CR ratio and the heat treatment temperature on hardness of EUROFER97 steel. Heat treatment was performed for 1 h in argon atmosphere.

As already shown by the plot in Figure 6, hardness of cold-rolled samples is always greater than that of the material prepared by the standard treatment. It decreases as heat treatment temperature increases and the change is more pronounced in the samples cold-rolled with greater CR ratios. This result is evident in Table 4 which reports the percentage softening values at the maximum temperature (750 °C) for different CR ratios. The softening percentage was calculated as the ratio between the hardness after 1 h at 750 °C and that of the as-deformed material.

Table 4. Softening percentage of EUROFER97 steel, in the temperature range of the annealing heat treatment from 400 °C to 750 °C.

CR Ratio %	20	40	50	60	80
Softening %	10.8	48.7	50.7	53	54.2

In the case of CR ratios of 60% and 80%, and for heat treatment temperatures above 650 °C a rapid degradation of hardness is observed with values lower than those of the steel in standard condition. The same is true for CR ratios of 40% and 50%, but for higher temperature (above 700 °C). On the contrary, for the CR ratio of 20%, the hardness stays above the standard value, independent of the heat treatment temperature.

After the heat treatment at 650 °C, the hardness is ~230 HV, i.e., significantly lower than that of the cold-rolled steel (~300 HV) but still 15% greater than steel after the standard preparation route (~200 HV).

For higher heat treatment temperatures (700 and 750 °C), abnormal grain growth takes place leading to hardness dropping below that of EUROFER97 prepared in standard conditions.

On the basis of the results displayed in Figure 12 some samples (CR: 80%, heat-treated at 400 °C, 500 °C, 600 °C and 650 °C) have been selected for tensile tests. The curves are reported in Figure 13 while Figure 14 displays the corresponding values of YS, UTS and A%. As expected, ultimate tensile stress (UTS) and yield stress (YS) decrease as temperature increases, while total elongation (A%) exhibits the opposite behavior.

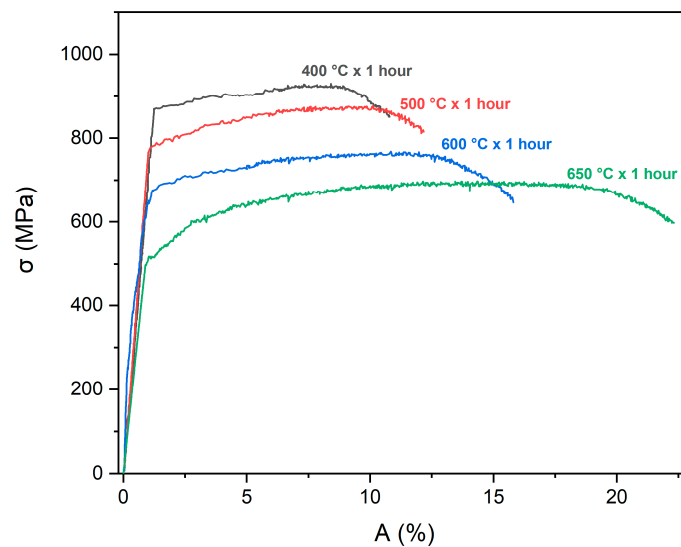


Figure 13. Tensile test curves of EUROFER97 steel cold rolled with CR of 80% and heat-treated at 400 °C, 500 °C, 600 °C and 650 °C for 1 h.

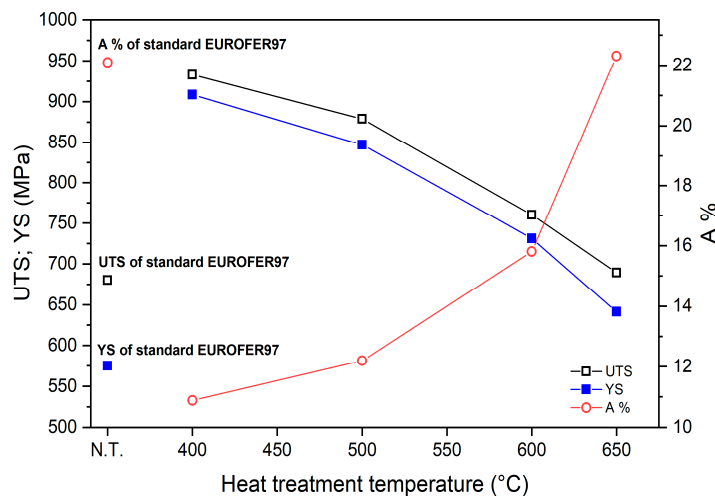


Figure 14. UTS, YS and A% of EUROFER97 steel cold rolled with CR of 80% and heat-treated at 400 °C, 500 °C, 600 °C and 650 °C for 1 h. The values of the steel prepared by standard treatment [23] are reported for comparison.

After the heat treatments at 400, 500 and 600 °C the values of YS and UTS are significantly larger than those of standard EUROFER97 [23] but such strengthening leads to lower ductility. On the contrary, the treatment at 650 °C increases YS of about 12% with a comparable total elongation. Therefore, this work demonstrated that it is possible to strengthen EUROFER97 steel without compromising its ductility. The result is quite promising for nuclear fusion applications and the completion of microstructural analyses and mechanical tests of all the prepared samples will enable determination of the most effective process parameters.

In general, grain refinement achieved either by the thermo-mechanical treatments proposed here or through a two-stage normalizing treatment refining the prior austenitic grain [51] seems a promising approach for improving strength without detrimental effects on ductility. A critical aspect emerging from the present work is the abnormal grain growth: its onset is favored by high treatment temperatures, and it leads to a drop in mechanical performance. The fast growth of few grains at the expenses of other grains can be explained by the presence of coincidence site lattice (CSL) special boundaries which have higher mobility than common boundaries [49] and by the coarsening of carbides.

4. Conclusions

This work reports preliminary results of an extended experimental campaign aimed at improving the strength of EUROFER97 steel through microstructure refining without introducing detrimental effects on its ductility. From the as-supplied material prepared through the standard treatment, 40 different groups of samples were obtained by combining cold rolling with five CR ratios and eight heat treatment temperatures. The results of microstructural examination and mechanical tests can be summarized as follows.

Cold rolling leads to grains of smaller size elongated along the rolling direction, the nearly random texture evolves towards a cubic [100] one with a secondary [211] component, and dislocation density increases. As expected, such microstructural changes, which are more relevant for greater CR ratios, induce a progressive strengthening of the material.

Recrystallization takes place in heat-treated samples with kinetics depending on treatment temperature and CR ratio. In the samples with CR of 80% at 650 °C, a population of equiaxed grains of sub-micrometric size was observed indicating that the primary recrystallization was completed. Higher treatment temperature in these samples induced abnormal grain growth.

The hardness of all the examined samples decreased as heat treatment temperature increased and the variation is more pronounced in the samples cold-rolled with greater CR ratios. Except for the samples deformed with CR ratio of 20%, it dropped below that of standard EUROFER97 for treatments above a critical temperature (700 °C if CR \geq 50%, 750 °C for lower CR).

On the basis of these results, tensile tests were performed on selected samples (CR ratio of 80%, treatment temperatures of 400, 500, 600 and 650 °C). In comparison to standard EUROFER97, the treatment at 650 °C leads to an increase in YS around 12% while the total elongation was nearly the same (~22%). On the contrary, after heat treatment at lower temperatures (400, 500 and 600 °C) YS and UTS were significantly larger but the steel had lower ductility.

In conclusion, this work demonstrated the feasibility to strengthen EUROFER97 steel without compromising its ductility. The result is promising for nuclear fusion applications and the completion of microstructural analyses and mechanical tests of all the prepared samples will allow us to identify the most effective process parameters.

Author Contributions: Conceptualization, G.S., R.M. and A.D.S.; methodology, G.S., R.M., A.D.S. and C.T.; formal analysis, G.S., R.M., S.M. and A.V.; supervision, R.M. and C.T.; draft paper preparation, G.S., R.M. and A.D.S.; final paper preparation, all authors. All authors have read and agreed to the published version of the manuscript.

Funding: This work was carried out within the framework of the EUROfusion Consortium and has received funding from the Euratom research and training program 2014–2018 and 2019–2020 under Grant Agreement No. 633053. The views and opinions expressed herein do not necessarily reflect those of the European Commission.

Institutional Review Board Statement: Not applicable.

Informed Consent Statement: Not applicable.

Data Availability Statement: The data presented in this study are available on request from the corresponding author.

Acknowledgments: The authors are grateful to Piero Plini of the Department of Industrial Engineering—University of Rome “Tor Vergata” for the assistance in sample preparation.

Conflicts of Interest: The authors declare no conflict of interest.

References

1. Rieth, M.; Schirra, M.; Falkenstein, A.; Graf, P.; Heger, S.; Kempe, H.; Lindau, R.; Zimmermann, H. *EUROFER 97 Tensile, Charpy, Creep and Structural Tests*; Report FZKA6911, Eurofusion Programme; Forschungszentrum Karlsruhe g.m.b.h.: Karlsruhe, Germany, 2003.
2. Zilnyk, K.D.; Oliveira, V.B.; Sandim, H.R.Z.; Möslang, A.; Raabe, D. Martensitic transformation in Eurofer-97 and ODS-Eurofer steels: A comparative study. *J. Nucl. Mater.* **2015**, *462*, 360–367. [[CrossRef](#)]
3. Huang, Q.; Baluc, N.; Dai, Y.; Jitsukawa, S.; Kimura, A.; Konys, J.; Kurtz, R.J.; Lindau, R.; Muroga, T.; Odette, G.R.; et al. Recent progress of R&D activities on reduced activation ferritic/martensitic steels. *J. Nucl. Mater.* **2013**, *442*, 2–8.
4. Sahoo, K.C.; Vanaja, J.; Parameswaran, P.; Vijayanand, V.D.; Laha, K. Effect of thermal ageing on microstructure, tensile and impact properties of reduced activated ferritic-martensitic steel. *Mater. Sci. Eng. A* **2017**, *686*, 54–64. [[CrossRef](#)]
5. Mao, C.; Liu, C.; Yu, L.; Li, H.; Liu, Y. Mechanical properties and tensile deformation behavior of a reduced activated ferritic-martensitic (RAFM) steel at elevated temperatures. *Mater. Sci. Eng. A* **2018**, *725*, 283–289. [[CrossRef](#)]
6. Donné, T. European Research Roadmap to the Realisation of Fusion Energy. In Proceedings of the 30th Symposium on Fusion Technology, Sicily, Italy, 16–21 September 2018.
7. Zinkle, S.J.; Möslang, A. Evaluation of irradiation facility options for fusion materials research and development. *Fusion Eng. Des.* **2013**, *88*, 472–482. [[CrossRef](#)]
8. Kohyama, A.; Hishinuma, A.; Gelles, D.S.; Klueh, R.L.; Dietz, W.; Ehrlich, K. Low-activation ferritic and martensitic steels for fusion application. *J. Nucl. Mater.* **1996**, *233–237*, 138–147. [[CrossRef](#)]
9. Di Schino, A.; Testani, C.; Pilloni, L. Effect of thermo-mechanical parameters on the mechanical properties of Eurofer97 steel for nuclear applications. *Open Eng.* **2018**, *8*, 349–353. [[CrossRef](#)]
10. Chen, J.; Liu, C.; Liu, Y.; Yan, B.; Li, H. Effects of tantalum content on the microstructure and mechanical properties of low-carbon RAFM steel. *J. Nucl. Mater.* **2016**, *479*, 295–301. [[CrossRef](#)]
11. Chen, J.; Liu, Y.; Liu, C.; Yan, B.; Li, H. Effects of tantalum on austenitic transformation kinetics of RAFM steel. *J. Iron Steel Res. Int.* **2017**, *24*, 705–710. [[CrossRef](#)]
12. Tavassoli, A.A.F.; Diegele, E.; Lindau, R.; Luzginova, N.; Tanigawa, H. Current status and recent research achievements in ferritic/martensitic steels. *J. Nucl. Mater.* **2014**, *455*, 269–276. [[CrossRef](#)]
13. Mergia, K.; Boukos, N. Structural, thermal, electrical and magnetic properties of Eurofer 97 steel. *J. Nucl. Mater.* **2008**, *373*, 1–8. [[CrossRef](#)]
14. Tavassoli, A.A.F.; Alamo, A.; Bedel, L.; Forest, L.; Gentzmittel, J.M.; Rensman, J.W.; Diegele, E.; Lindau, R.; Schirra, M.; Schmitt, R.; et al. Materials design data for reduced activation martensitic steel type EUROFER. *J. Nucl. Mater.* **2004**, *329–333*, 257–262. [[CrossRef](#)]
15. Hoffmann, J.; Rieth, M.; Commin, L.; Fernández, P.; Roldán, M. Improvement of reduced activation 9%Cr steels by ausforming. *Nucl. Mater. Energy* **2016**, *6*, 12–17. [[CrossRef](#)]
16. Stornelli, G.; Rallini, M.; Testani, C.; Montanari, R.; Di Schino, A. Effetto di trattamenti termomeccanici su acciaio EUROFER97 per applicazioni in reattori a fusione nucleare. *La Metall. Ital.* **2020**, *112*, 34–44.
17. Chen, X.; Bhattacharya, A.; Sokolov, M.A.; Clowers, L.N.; Yamamoto, Y.; Graening, T.; Linton, K.D.; Katoh, Y.; Rieth, M. Mechanical properties and microstructure characterization of Eurofer97 steel variants in EUROfusion program. *Fusion Eng. Des.* **2019**, *146*, 2227–2232. [[CrossRef](#)]
18. Gaganidze, E.; Gillemot, F.; Szenthe, I.; Gorley, M.; Rieth, M.; Diegele, E. Development of EUROFER97 database and material property handbook. *Fusion Eng. Des.* **2018**, *135*, 9–14. [[CrossRef](#)]
19. Montanari, R.; Filacchioni, G.; Iacovone, B.; Plini, P.; Riccardi, B. High temperature indentation tests on fusion reactor candidate materials. *J. Nucl. Mater.* **2007**, *367–370*, 648–652. [[CrossRef](#)]
20. Stornelli, G.; Montanari, R.; Testani, C.; Pilloni, L.; Napoli, G.; Di Pietro, O.; Di Schino, A. Microstructure Refinement Effect on EUROFER 97 Steel for Nuclear Fusion Application. *Mater. Sci. Forum* **2021**, *1016*, 1392–1397. [[CrossRef](#)]

21. Puype, A.; Malerba, L.; De Wispelaere, N.; Petrov, R.; Sietsma, J. Effect of processing on microstructural features and mechanical properties of a reduced activation ferritic/martensitic EUROFER steel grade. *J. Nucl. Mater.* **2017**, *494*, 1–9. [[CrossRef](#)]
22. Montanari, R.; Filacchioni, G.; Riccardi, B.; Tata, M.E.; Costanza, G. Characterization of EUROFER 97 TIG-welded joints by FIMEC indentation tests. *J. Nucl. Mater.* **2004**, *1529*, 329–333. [[CrossRef](#)]
23. Lindau, R.; Möslang, A.; Rieth, M.; Klimiankou, M.; Materna-Morris, E.; Alamo, A.; Tavassoli, A.A.F.; Cayron, C.; Lancha, A.M.; Fernandez, P.; et al. Present development status of EUROFER and ODS-EUROFER for application in blanket concepts. *Fusion Eng. Des.* **2005**, *75–79*, 989–996. [[CrossRef](#)]
24. Coppola, R.; Klimenkov, M. Dose Dependence of Micro-Voids Distributions in Low-Temperature Neutron Irradiated Eurofer97 Steel. *Metals* **2019**, *9*, 552. [[CrossRef](#)]
25. Roldán, M.; Fernández, P.; Rams, J.; Sánchez, F.J.; Gómez-Herrero, A. Nanoindentation and TEM to Study the Cavity Fate after Post-Irradiation Annealing of He Implanted EUROFER97 and EU-ODS EUROFER. *Micromachines* **2018**, *9*, 633. [[CrossRef](#)] [[PubMed](#)]
26. Fu, J.; Brouwer, J.; Hendrikx, R.; Richardson, I.; Hermans, M. Microstructure characterisation and mechanical properties of ODS Eurofer steel subject to designed heat treatments. *Mater. Sci. Eng. A* **2020**, *770*, 138568. [[CrossRef](#)]
27. Testani, C.; Di Nunzio, P.E.; Salvatori, I. Manufacturing of ODS RAFM Steel: Mechanical and Microstructural Characterization. *Mater. Sci. Forum* **2016**, *879*, 1639–1644. [[CrossRef](#)]
28. De Sanctis, M.; Fava, A.; Lovicu, G.; Montanari, R.; Richetta, M.; Testani, C.; Varone, A. Mechanical characterization of a nano-ODS steel prepared by low-energy mechanical alloying. *Metals* **2017**, *7*, 283. [[CrossRef](#)]
29. Mateus, R.; Carvalho, P.A.; Nunes, D.; Alves, L.C.; Franco, N.; Correia, J.B.; Alves, E. Microstructural characterization of the ODS Eurofer 97 EU-batch. *Fusion Eng. Des.* **2011**, *86*, 2386–2389. [[CrossRef](#)]
30. Cabet, C.; Dalle, F.; Henry, J.; Gaganidze, E.; Tanigawa, H. Ferritic-martensitic steels for fission and fusion applications. *J. Nucl. Mater.* **2019**, *523*, 510–537. [[CrossRef](#)]
31. De Sanctis, M.; Fava, A.; Lovicu, G.; Montanari, R.; Richetta, M.; Testani, C.; Varone, A. Temperature Dependent Mechanical Behavior of ODS Steels. *Mater. Sci. Forum* **2018**, *941*, 257–262. [[CrossRef](#)]
32. Fava, A.; Montanari, R.; Richetta, M.; Testani, C.; Varone, A. Analysis of Strengthening Mechanisms in Nano-ODS Steel Depending on Preparation Route. *J. Mater. Sci. Eng.* **2018**, *7*, 2169. [[CrossRef](#)]
33. Schaeublin, R.; Leguey, T.; Spätig, P.; Baluc, N.; Victoria, M. Microstructure and mechanical properties of two ODS ferritic/martensitic steels. *J. Nucl. Mater.* **2002**, *307–311*, 778–782. [[CrossRef](#)]
34. Zhou, J.H.; Shen, Y.F.; Jia, N. Strengthening mechanisms of reduced activation ferritic/martensitic steels: A review. *Int. J. Miner. Metall. Mater.* **2021**, *28*, 335–348. [[CrossRef](#)]
35. Gondi, P.; Montanari, R. On the Cr distribution in MANET steel. *Phys. Stat. Solid. A* **1992**, *131*, 465–480. [[CrossRef](#)]
36. Fava, A.; Montanari, R.; Varone, A. Mechanical Spectroscopy Investigation of Point Defect-Driven Phenomena in a Cr Martensitic Steel. *Metals* **2018**, *8*, 870. [[CrossRef](#)]
37. Bolli, E.; Fava, A.; Ferro, P.; Kaciulis, S.; Mezzi, A.; Montanari, R.; Varone, A. Cr Segregation and Impact Fracture in a Martensitic Stainless Steel. *Coatings* **2020**, *10*, 843. [[CrossRef](#)]
38. Zhou, W.; Yu, J.; Lin, J.; Dean, T.A. Manufacturing a curved profile with fine grains and high strength by differential velocity sideways extrusion. *Int. J. Mach. Tools. Manuf.* **2019**, *140*, 77–88. [[CrossRef](#)]
39. Zhou, W.; Yu, J.; Lu, X.; Lin, J.; Dean, T.A. A comparative study on deformation mechanisms, microstructures and mechanical properties of wide thin-ribbed sections formed by sideways and forward extrusion. *Int. J. Mach. Tools. Manuf.* **2021**, *168*, 103771. [[CrossRef](#)]
40. Pickering, F.B.; Gladman, T. *Metallurgical Developments in Carbon Steels*; Special Report No. 81; Iron and Steel Institute: London, UK, 1963.
41. Di Schino, A.; Alleva, L.; Guagnelli, M. Microstructure Evolution during Quenching and Tempering of Martensite in a Medium C Steel. *Mater. Sci. Forum* **2012**, *715–716*, 860–865. [[CrossRef](#)]
42. Di Schino, A. Manufacturing and application of stainless steels. *Metals* **2020**, *10*, 327. [[CrossRef](#)]
43. Beyerlein, I.J.; Caro, A.; Demkowicz, M.J.; Mara, N.A.; Misra, A.; Uberuaga, B.P. Radiation damage tolerant nanomaterials. *Mater. Today* **2013**, *16*, 443–449. [[CrossRef](#)]
44. Song, M.; Wu, Y.D.; Chen, D.; Wang, X.M.; Sun, C.; Yu, K.Y.; Chen, Y.; Shao, L.; Yang, Y.; Hartwig, K.T.; et al. Response of equal channel angular extrusion processed ultrafine-grained T91 steel subjected to high temperature heavy ion irradiation. *Acta Mater.* **2014**, *74*, 285–295. [[CrossRef](#)]
45. Di Schino, A.; Gaggiotti, M.; Testani, C. Heat Treatment Effect on Microstructure Evolution in a 7% Cr Steel for Forging. *Metals* **2020**, *10*, 808. [[CrossRef](#)]
46. Mancini, S.; Langellotto, L.; Di Nunzio, P.E.; Zitelli, C.; Di Schino, A. Defect Reduction and Quality Optimization by Modeling Plastic Deformation and Metallurgical Evolution in Ferritic Stainless Steels. *Metals* **2020**, *10*, 186. [[CrossRef](#)]
47. Cristalli, C.; Piloni, L.; Tassa, O.; Bozzetto, L. Mechanical properties of several newly produced RAFM steels with Tungsten content in the range of 2 wt%. *Nucl. Mater. Energy* **2020**, *25*, 100793. [[CrossRef](#)]
48. Cristalli, C.; Piloni, L.; Tassa, O.; Bozzetto, L.; Sorci, R.; Masotti, L. Development of innovative steels and thermo-mechanical treatments for DEMO high operating temperature blanket options. *Nucl. Mater. Energy* **2018**, *16*, 175–180. [[CrossRef](#)]

49. Oliveira, V.B.; Sandim, H.R.Z.; Raabe, D. Abnormal grain growth in Eurofer-97 steel in the ferrite phase field. *J. Nucl. Mater.* **2017**, *485*, 23–38. [[CrossRef](#)]
50. Lan, H.F.; Liu, W.J.; Liu, X.H. Ultrafine ferrite grains produced by tempering cold-rolled martensite in low carbon and microalloyed steels. *ISIJ Int.* **2007**, *47*, 1652–1657. [[CrossRef](#)]
51. Karthikeyan, T.; Thomas Paul, V.; Saroja, S.; Moitra, A.; Sasikala, G.; Vijayalakshmi, M. Grain refinement to improve impact toughness in 9Cr-1Mo steel through a double austenitization treatment. *J. Nucl. Mater.* **2011**, *419*, 256–262. [[CrossRef](#)]
52. Pilloni, L.; Cristalli, C.; Tassa, O.; Salvatori, I.; Storai, S. Grain size reduction strategies on Eurofer. *Nucl. Mater. Energy* **2018**, *17*, 129–136. [[CrossRef](#)]
53. Stornelli, G.; Di Schino, A.; Montanari, R.; Testani, C.; Varone, A.; Mancini, S. Work-Hardening Behavior of Cold Rolled EUROFER97 Steel for Nuclear Fusion Applications. *Mater. Proc.* **2021**, *3*, 21. [[CrossRef](#)]
54. Williamson, G.K.; Smallman, R.E., III. Dislocation densities in some annealed and cold-worked metals from measurements on the X-ray Debye-Scherrer spectrum. *Philos. Mag.* **1956**, *1*, 34–46. [[CrossRef](#)]
55. Gondi, P.; Montanari, R.; Sili, A. Small scale non-destructive stress-strain and creep tests feasible during irradiation. *J. Nucl. Mater.* **1994**, *1688*, 212–215.
56. Riccardi, B.; Montanari, R.; Moreschi, L.F.; Sili, A.; Storai, S. Mechanical characterization of fusion materials by indentation test. *Fusion Eng. Des.* **2001**, *755*, 58–59.
57. Klimenkov, M.; Lindau, R.; Materna-Morris, E.; Möslang, A. TEM characterization of precipitates in EUROFER 97. *Prog. Nucl. Energy* **2012**, *57*, 8–13. [[CrossRef](#)]
58. Fernández, P.; Lancha, A.M.; Lapeña, J.; Hernández-Mayoral, M. Metallurgical characterization of the reduced activation ferritic/martensitic steel Eurofer'97 on as-received condition. *Fusion Eng. Des.* **2001**, *58–59*, 787–792. [[CrossRef](#)]
59. JCPDS. *International Centre for Diffraction Data*; JCPDS: Newtown Square, PA, USA, 1907. Available online: <https://www.icdd.com/> (accessed on 17 March 2021).